iScience, Volume *26*

Supplemental information

BRPF1 bridges H3K4me3 and H3K23ac in human embryonic stem cells and is essential to pluripotency

Cong Zhang, Huaisong Lin, Yanqi Zhang, Qi Xing, Jingyuan Zhang, Di Zhang, Yancai Liu, Qianyu Chen, Tiancheng Zhou, Junwei Wang, Yongli Shan, and Guangjin Pan

Figure S1

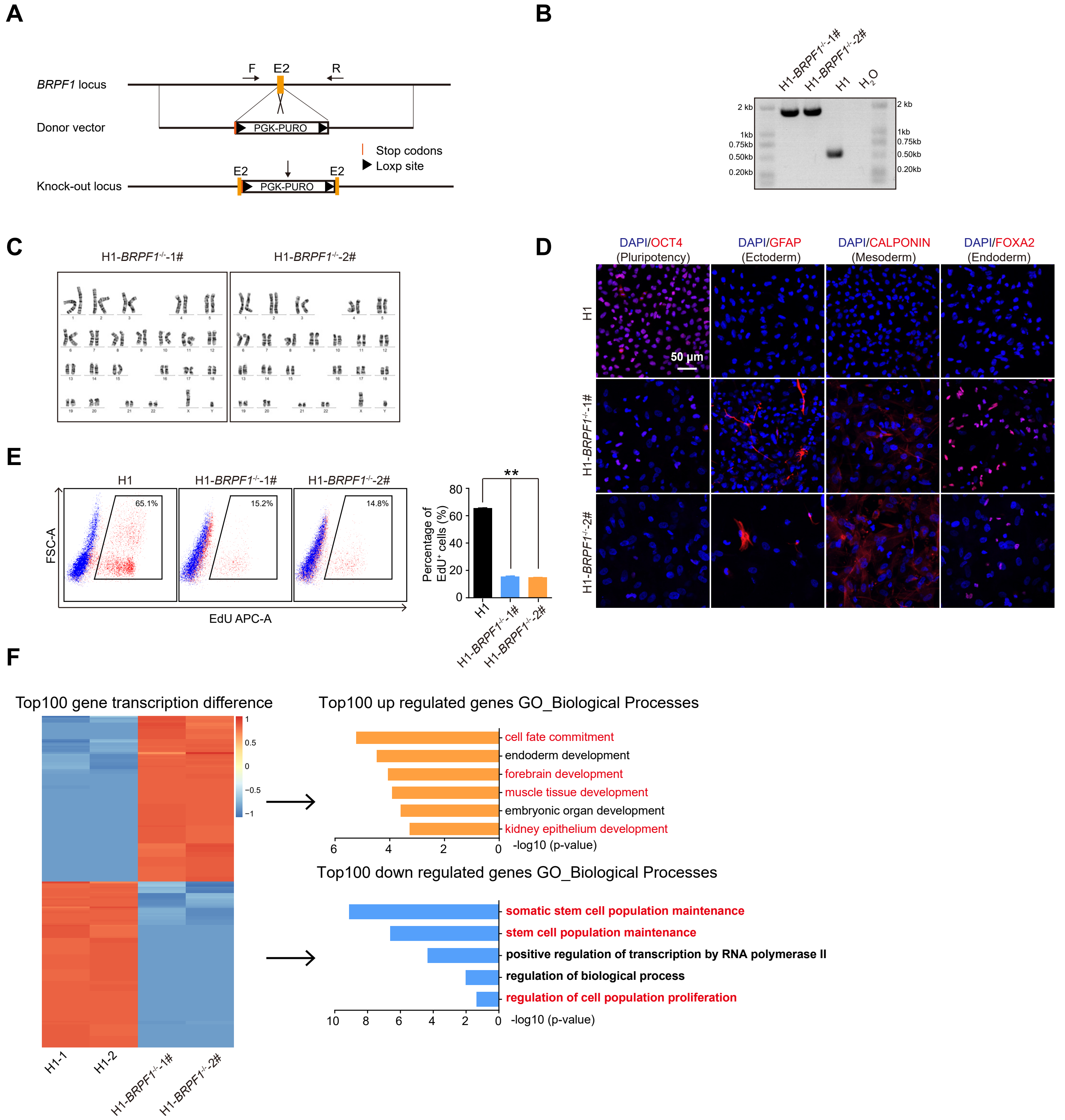

Figure S1. BRPF1 is an indispensable gene for the pluripotency and self-renewal of hESCs, related to Figure 1.

(A) Overview of the BRPF1 targeting strategy. sgRNA was designed, and a homologous targeting vector containing a puromycin resistance cassette was constructed according to the BRPF1 gene. (B) PCR identification of WT and two BRPF1$^{-/-}$ H1 hESC clones. WT hESCs served as a negative control. (C) Karyotype in BRPF1$^{-/-}$ H1 hESCs. (D) Immunostaining of the pluripotency and lineage markers OCT4 (pluripotency), GFAP (ectoderm), CALPONIN (mesoderm), and FOXA2 (endoderm) in WT and two BRPF1$^{-/-}$ H1 hESC clones. Scale bar, 50 μm. (E) EdU incorporation assay in WT and two BRPF1$^{-/-}$ H1 hESC clones. The significance level was determined by unpaired two-tailed Student's t tests. **, P < 0.01. The data represent the mean ± SD (standard deviation) from three independent repeats (n=3). (F) Heatmap and GO analysis of the top 100 genes up- or down-regulated in two BRPF1$^{-/-}$ H1 hESC clones compared with WT H1 hESCs. All error bars throughout the figure represent the SD (standard deviation) from three independent replicates (n = 3).

Figure S2

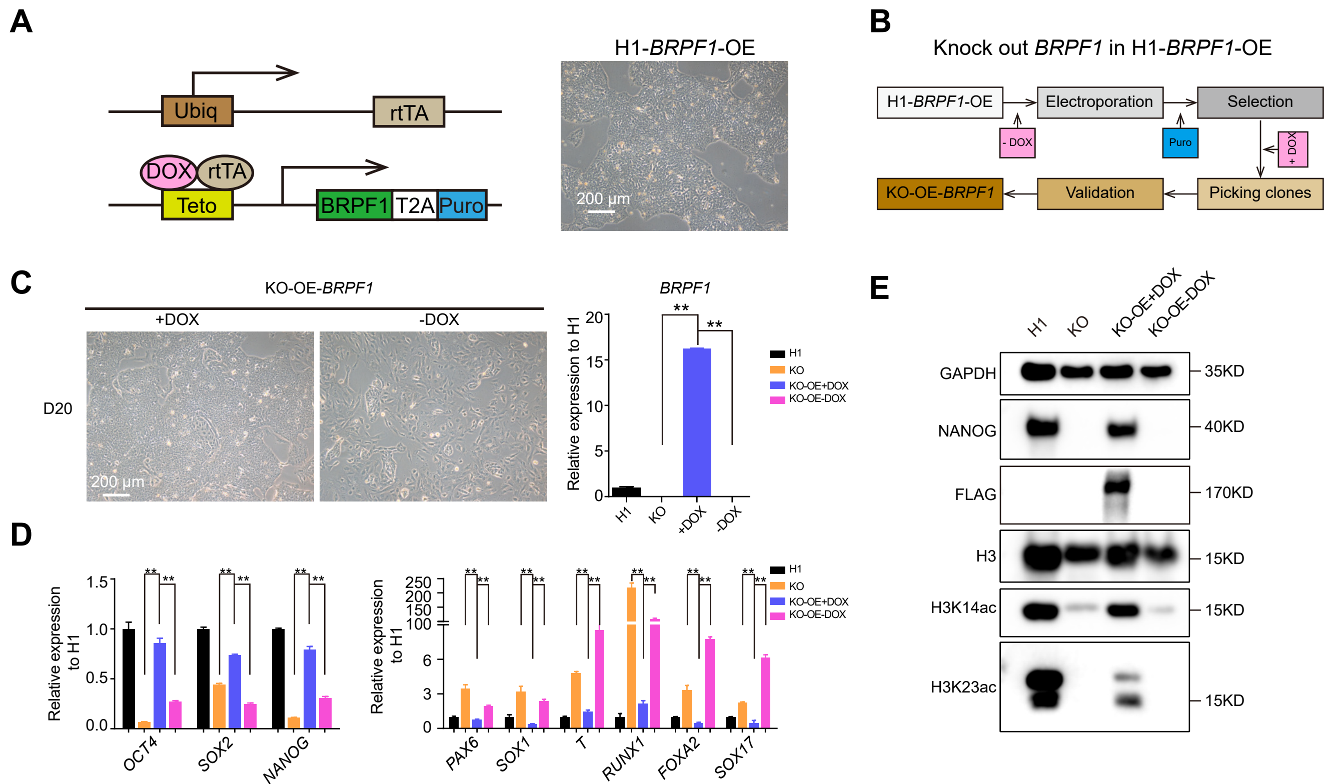

Figure S2. Inducible expression of BRPF1 complements the BRPF1$^{-/-}$ hESCs phenotype, related to Figure 2.

(A) Diagram of the lentiviral-based inducible system for BRPF1 expression (H1-BRPF1-OE). BRPF1 expression was controlled by DOX treatment. (B) Schematic of BRPF1 knockout in H1 hESCs with BRPF1 over expression (KO-OE-BRPF1). (C) The morphology of BRPF1$^{-/-}$ H1 hESCs with BRPF1 over-expression (+DOX) or no (-DOX) was shown. Scale bar, 200 μm. The expression of BRPF1 was examined in the indicated cells by qRT-PCR. The significance level was determined by unpaired two-tailed Student's t tests. **, $P < 0.01$. The data represent the mean ± SD (standard deviation) from three independent repeats (n=3). (D) Examination of the expression of the selected pluripotent and lineage genes in the indicated cells by qRT-PCR. The significance level was determined by unpaired two-tailed Student's t tests. **, $P < 0.01$. The data represent the mean ± SD (standard deviation) from three independent repeats (n=3). (E) Western blot of NANOG, BRPF1 (FLAG), H3K14ac or H3K23ac in the indicated cells. All error bars throughout the figure represent the SD (standard deviation) from three independent replicates (n = 3).

Figure S3

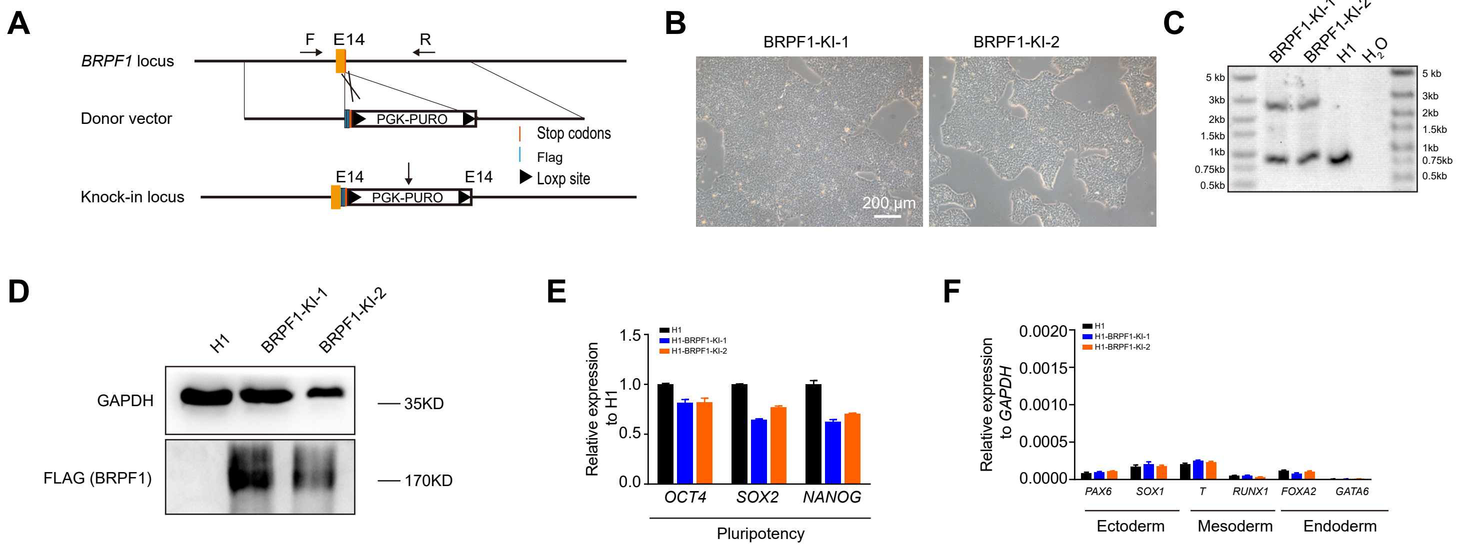

Figure S3. Knock in triple-FLAG into BRPF1 locus in hESCs, Related to Figure 4.

(A) Overview of the BRPF1 locus knock-in (KI) triple-FLAG strategy. (B) Morphology of BRPF1-KI H1 hESCs. Scale bar, 200 μm. (C) PCR identification in WT and two BRPF1-KI H1 hESC clones. WT hESCs served as a negative control. (D) GAPDH protein and FLAG tag were examined in WT and two BRPF1-KI H1 hESC clones by western blot. (E-F) Examination of the expression of the selected (E) pluripotent and (F) lineage genes in WT and two BRPF1-KI H1 hESC clones.

Figure S4

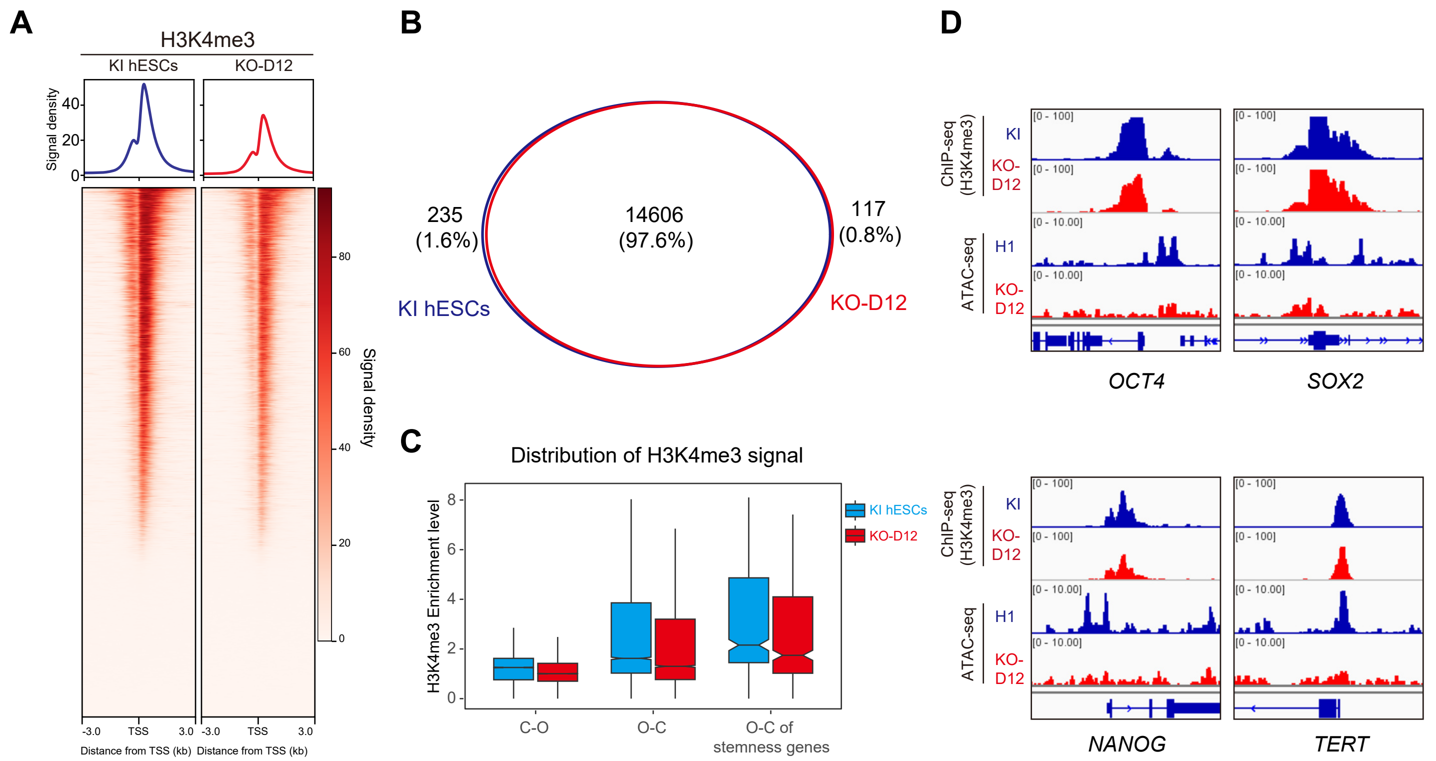

Figure S4. Similar localization of H3K4me3 between WT and BRPF1$^{-/-}$ hESCs, Related to Figure 4.

(A) Heatmap and signal densities of H3K4me3 associated genes in KI and BRPF1$^{-/-}$ hESCs from ChIP-seq. (B) Venn diagram for H3K4me3 associated genes in the indicated cells. (C) Enrichment of H3K4me3 associated with different regions. ”C-O” represents regions of close to open; ”O-C” represents regions of open to close; ”O-C of stemness genes” represents regions of open to close in stemness genes. (D) Genomic views of H3K4me3 enrichment and ATAC-seq analysis in the indicated WT and BRPF1$^{-/-}$ hESCs.